ANALYSIS OF LAND COVER CHANGES TO INCREASE LAND SURFACE TEMPERATURE IN SURABAYA USING LANDSAT SATELLITE

Shanas Septy Prayuda[1,2*], Maritha Nilam Kusuma[1]
[1]Masters in Environmental Engineering, Faculty of Civil Engineering and Planning, Institut Teknologi Adhi Tama Surabaya
[2]Juanda Meteorological Station, Sidoarjo
*****E-mail: shanas.prayuda@gmail.com

Article submitted: November 22, 2022 Article revised: May 18, 2023 Article accepted: January 19, 2024

ABSTRACT

Surabaya has experienced very significant development in the last few decades. Changes in land use will cause the Urban Heat Island phenomenon. This study aims to determine how far the impact of land cover changes on the increase in surface temperature in the Surabaya. The use of Landsat satellite imagery is considered very effective in describing land cover and surface temperature because it has good spatial resolution and long data availability. During 1991 – 2020 there was a significant decrease in the amount of vegetation by 24.3%, decrease in the number of water bodies by 4.9%, and increase in the number of buildings by 29.2%. The average increase in Land Surface Temperatures was 1.40^{o}C between decades 2 and 1, and an increase of 2.19^{o}C between decades 3 and 2. The development of Surabaya began in the city center and then developed mainly in the west and east. The urban development model is consistent with the pattern of land surface temperature changes. Each type of land cover has special characteristics on the value of NDVI, NDBI, and surface temperature. Changes in cover from water bodies to buildings have the highest contribution to increasing the land surface temperature. There was a significant increase in hotspots in decade 3 in Surabaya which indicated an increasingly severe UHI phenomenon.

Keywords: UHI, Land Cover, NDVI, NDBI, LST

1. Introduction

Urban Heat Island (UHI) is an indication of local warming in urban areas when compared to the surrounding environment [1]. UHI is caused by infrastructure development such as buildings, roads, and so on [2]. The infrastructure development will change the land cover which causes changes to the dynamics of the atmosphere around the area.

Currently, there have been many studies on UHI based on observations of Land Surface Temperatures (LST) obtained from remote sensing data [3]–[6]. In addition, an analysis of the UHI phenomenon can also be carried out by comparing temperatures in urban and rural areas using automated observation stations [7], [8]. The use of different analytical methods will have their respective advantages and disadvantages. Analysis using ground observations has the advantages of temporal resolution, high historical time series, and data interpretation that can describe actual conditions. Ground observation in the field has the disadvantage of low spatial resolution because it is limited by the number of existing observation stations [9]. On the other way, UHI analysis using remote sensing such as satellites will have a high spatial resolution when compared to ground observations but has a lack of temporal resolution.

Previous studies have used many remote sensing indices such as the Normalized Difference Built-up Index (NDBI) and the Normalized Difference Vegetation Index (NDVI) to map land cover types [10], [11]. NDVI itself can generally describe the vegetation or greenness of an area. This method is often used in research as an alternative to describing vegetation in an area and is the most commonly used index to examine spatial and temporal variations in surface temperature [12], while the NDBI is an index that states the built-up area. These two methods are the most commonly used spatial analysis techniques, including the urban-rural gradient analysis approach [13], [14].

Surabaya the capital of the province of East Java is a metropolitan city with a very rapid development rate. Previous studies have shown that metropolitan cities in the world have a significant UHI effect and land cover changes in urban areas greatly affect UHI patterns [1]. UHI will exacerbate the impact of global warming in urban areas with dense buildings and less vegetation. Knowledge of UHI is useful for various geoscience fields such as urban climatology, environmental change, and human-environment interactions, and most importantly for planning and management practices[15].

This study focuses on assessing the effect of land use change on LST in Surabaya by analyzing the surface temperature approach by the Landsat satellite to obtain a good spatial study. Land cover analysis is divided into 3 types of land cover, namely vegetation,

buildings, and water bodies. The three types of land cover were chosen because they have a special reflectivity value for each type. The results of this study can provide a better understanding of the relationship between environmental and human conditions on urban surface temperature variations, which can facilitate environmental management and urban planning to reduce the impact of UHI in urban areas.

2. Methods

The research was conducted in Surabaya which is the largest metropolitan city in East Java. This study relates the relationship between land cover change and the increase in LST during 1991-2020 and is analyzed every decade. Furthermore, the analysis in 1991-2000 is called decade 1, 2001-2010 is called decade 2, and 2011-2020 is called decade 3. The use of Landsat satellite imagery to determine the increase in LST that occurs spatially and with long temporal resolution. The conceptual framework of this research is in Figure 1.

Landsat 5, 7, and 8 Path 118 Row 65 satellite image data 1991-2020 from the United States Geological Survey (USGS) which can be downloaded from the website http://earthexplorer.usgs.gov/. This study also used satellite photo data and aerial photos taken from various sources to verify land cover classification results from Landsat satellite imagery.
The research begins with the process of collecting Landsat satellite image data with coverage of Surabaya. The Landsat satellite image was processed nd resampled to a resolution of 30 m. Landsat satellite images are filtered based on the amount of cloud cover <10% to avoid too many clouds affecting the results of Landsat satellite imagery observations. Then radiometric correction is performed to eliminate the influence of atmospheric disturbances and produce a better image. The last step in the pre-processing phase is cloud masking to get better data quality. The corrected satellite image data is processed to produce the land cover, NDVI (1), NDBI (2), and LST.

$$NDVI = \frac{NIR-RED}{NIR+RED} \quad (1)$$

$$NDBI = \frac{SWIR-NIR}{SWIR+NIR} \quad (2)$$

NIR is the near-infrared band, RED is the red band of the satellite, and SWIR is short-wave infrared. The surface temperature product can be obtained from Landsat satellite thermal sensor data. The first step is to change the Digital Number (DN) value to a spectral radian value (3).

$$L\lambda = \frac{L_{max}-L_{min}\ x\ (QCAL-QCAL_{min})}{QCAL_{max}-QCAL_{min}} - L_{min} \quad (3)$$

Lλ is a certain spectral radian band (watt*m^{-2}*ster^{-1}*µm^{-1}), $QCAL_{min}$ and $QCAL_{max}$ are the minima and maximum digital number values in the image; L_{max} and L_{min} are spectral radian values at $QCAL_{max}$ and $QCAL_{min}$ in watt*m^{-2}*ster^{-1}*µm^{-1}. The next step is to change the spectral radian value that has been obtained previously into brightness temperature using equation 4.

$$Tb = \frac{K_2}{ln\left(\frac{K_1}{L\lambda}+1\right)} \quad (4)$$

Tb is the brightness temperature in Kelvin, Lλ is the spectral radian (watt*m^{-2}*ster^{-1}*µm^{-1}), K_1 and K_2 are the calibration constants on the Landsat satellite. Then use the equation of the vegetation fraction (Pv) to get the surface emissivity value, with equation 5.

$$P_v = \left[\frac{NDVI-NDVI_{min}}{NDVI_{max}-NDVI_{min}}\right]^2 \quad (5)$$

The next step is to find the surface emissivity value to reduce errors in estimating the surface temperature. Emissivity (ε) is shown by equation 6.

$$\varepsilon = 0.004 \times Pv + 0.986 \quad (6)$$

The last step is to calculate the surface temperature using equation 7.

$$LST = \frac{Tb}{\left(1+w\frac{Tb}{p}l\ (\varepsilon)\right)} - 273.15 \quad (7)$$

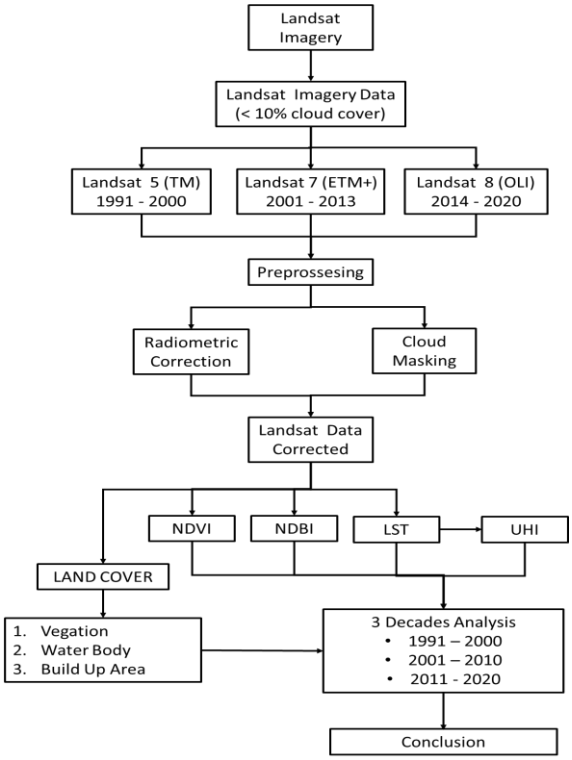

Figure 1. Research Flowchart

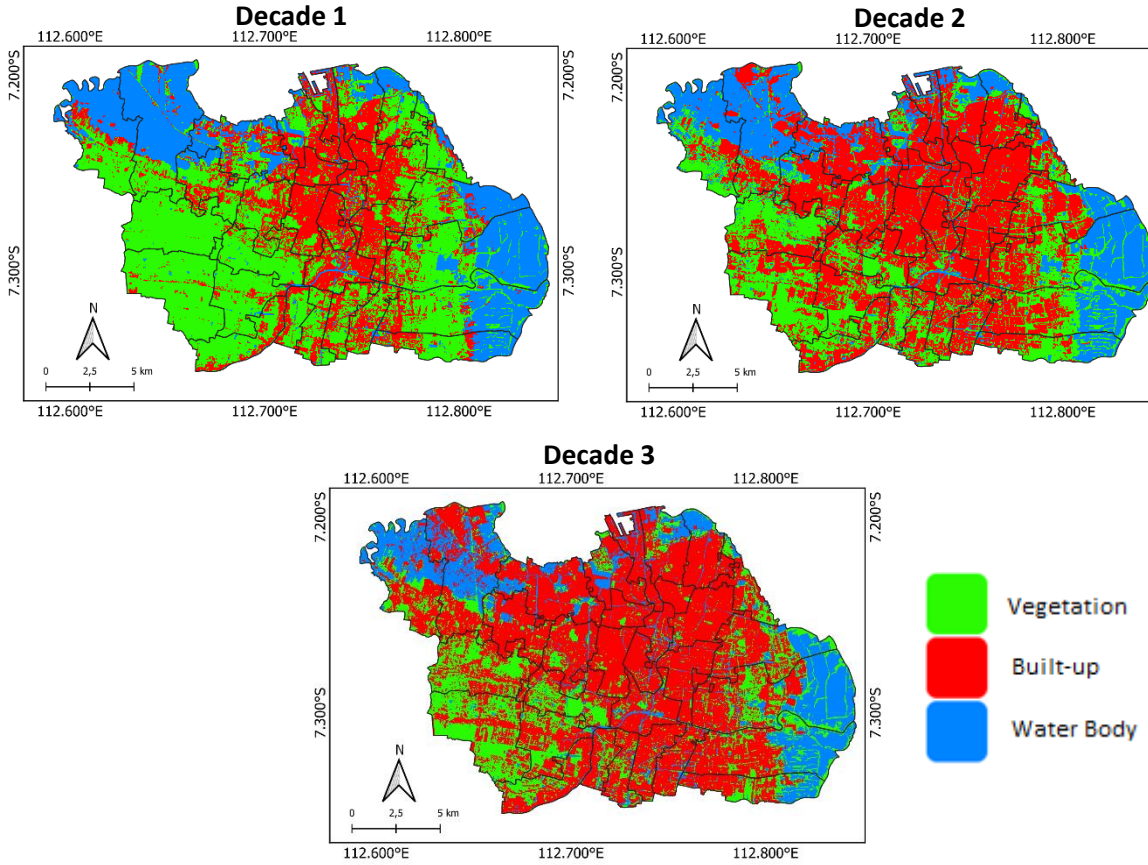

Figure 2. Surabaya Land Cover Classification

w is the wavelength of the beam, p=h*c/σ = 1.438×10−2 m K (σ is Boltzmann's constant, h is Planck's constant, and c is the speed of light). At the end of the equation, subtract 273.15 to get units of degrees Celsius. Landsat satellite data processing is carried out using the composite method in each decade, using the median concept. The product values collected at each pixel are sorted and the middle value is taken to reduce the extreme values that occur.

The UHI_{index} is used to describe the UHI phenomenon more intensively. UHI_{index} is calculated using the equation 8[16].

$$UHI_{index} = \frac{LST_i - LST_{min}}{LST_{max} - LST_{min}} \quad (8)$$

LST_i is the LST of grid points in the spatial distribution of LST, LSTmax and min are the maximum and minimum LST in the study area.

The land cover area was obtained using machine learning methods. The classification and Regression Trees (CART) algorithm is used based on the available bands on the Landsat satellite. The classification process is carried out using the type of supervised classification, which is a classification method using samples to label a class. Class determination is based on the similarity of reflectance and absorption characteristics of objects to electromagnetic waves. CART can analyze complex data and provides an informative way of viewing the results in the form of a decision tree. In addition, CART can handle multiple response variables [17].

3. Result and Discussion

Land Cover Classification. In this study, land cover classification is divided into 3 types, namely vegetation, buildings, and water bodies. The results of land cover accuracy using 100 sample points in the city of Surabaya are 96% (Table 2).

These results are considered very good in representing the actual land cover of the city of Surabaya. Landsat satellites detect well areas of buildings and water bodies. In the vegetation area, the Landsat satellite still detects 2 samples of buildings and 2 samples of water bodies. The development of urbanization in the Surabaya area is very fast in the range of 1991-2020. Significant land cover changes were observed, from vegetation to building areas (Figure 2). The development of Surabaya is centered on the central area and develops in a north-south direction and is more dominant in a west-east direction until 2020. In addition, the distribution of water bodies in the Surabaya tends to be on the east, north, and west sides which are pond areas.

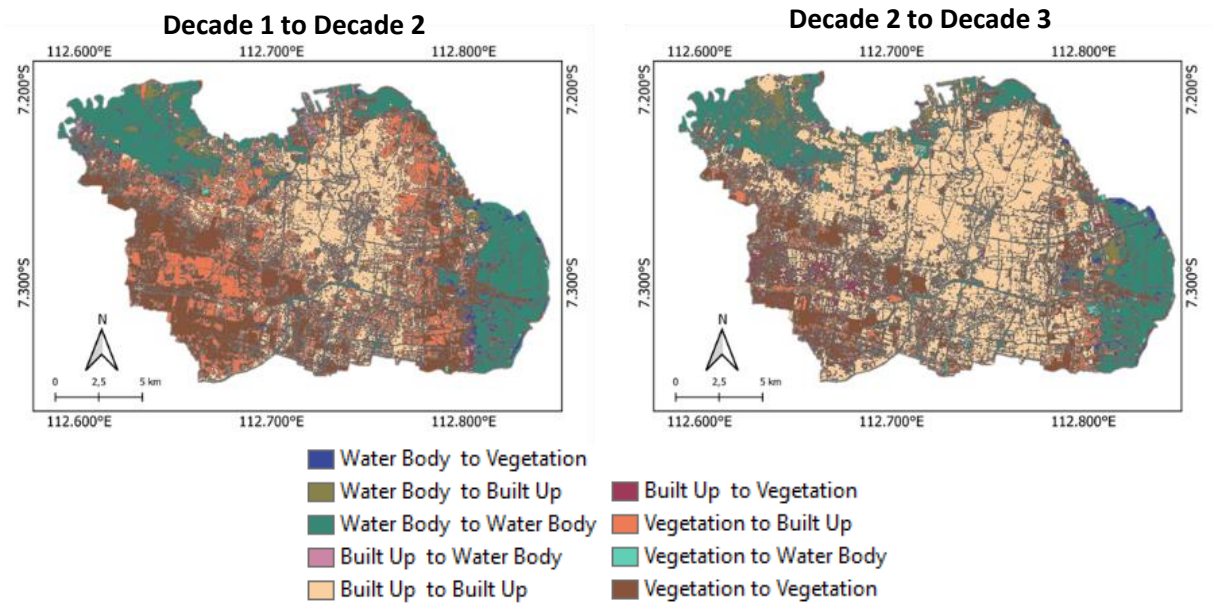

Figure 3. Spatial Distribution of Land Cover Changes in Surabaya.

Table 1. Changes in Land Cover Area Between Decades.

Land Cover	Area (km^2)	
	Decade 1 to Decade 2	Decade 2 to Decade 3
Vegetation to Vegetation	77,30560199	56,06689484
Vegetation to Built-up	76,29413813	32,45451193
Vegetation to Water Body	6,51615991	10,49029742
Built up to Vegetation	10,6153932	13,86078616
Built up to Built-up	75,82810571	142,1358162
Built up to Water Body	6,104067788	3,736806423
Water Body to Vegetation	11,07762442	8,267100133
Water Body to Built-up	7,606643678	16,43192142
Water Body to Water Body	61,1824217	49,08975154

Table 2. Land Cover Accuracy

Land Cover		Ground Observation		
		Vegetation	Built up	Water
Landsat	Vegetation	26	2	2
	Built up	0	40	0
	Water	0	0	30

The area of vegetation, buildings, and water bodies in the first decade is 160.117 km^2, 92.491 km^2, and 80.179 km^2 respectively, then in the second decade the area is 99.157 km^2, 158.590 km^2, and 75.041 km^2, and in the third decade, the area is 79.111 km^2, 189.721 km^2, and 63.956 km^2. In decade 1 the amount of vegetation still dominates with a percentage of 48.11% of the area of Surabaya and is replaced by buildings that dominate in decade 2 with a percentage of 30.84% area and in decade 3 more than half the area of Surabaya is the built-up area (57.01%). Vegetation area is decreasing every decade, with a decrease in the area of 38.072 km^2 between decades 2 and 1 and 20,047 km^2 between decades 3 and 2, then a significant increase in the area of built-up land by 66.098 km^2 between decades 2 and 1 and an increase in a building area of 31.131 km^2 between decades 3 and 2. In contrast to the land cover of vegetation and building types, water bodies experienced a smaller decrease in the area of 5.138 km^2 between decades 2 and 1 and 11.085 km2 between decades 3 and 2. The development of Surabaya as a metropolitan city was rated very quickly. The most significant development was carried out in 2001-2010 with changes in vegetation to buildings covering an area of 76.29 km^2 (Table 1). Several areas have changed from buildings to vegetation with an area of 10.62 km^2 in decade 1 to decade 2 and 13.86 km^2 in decade 2 to decade 3.

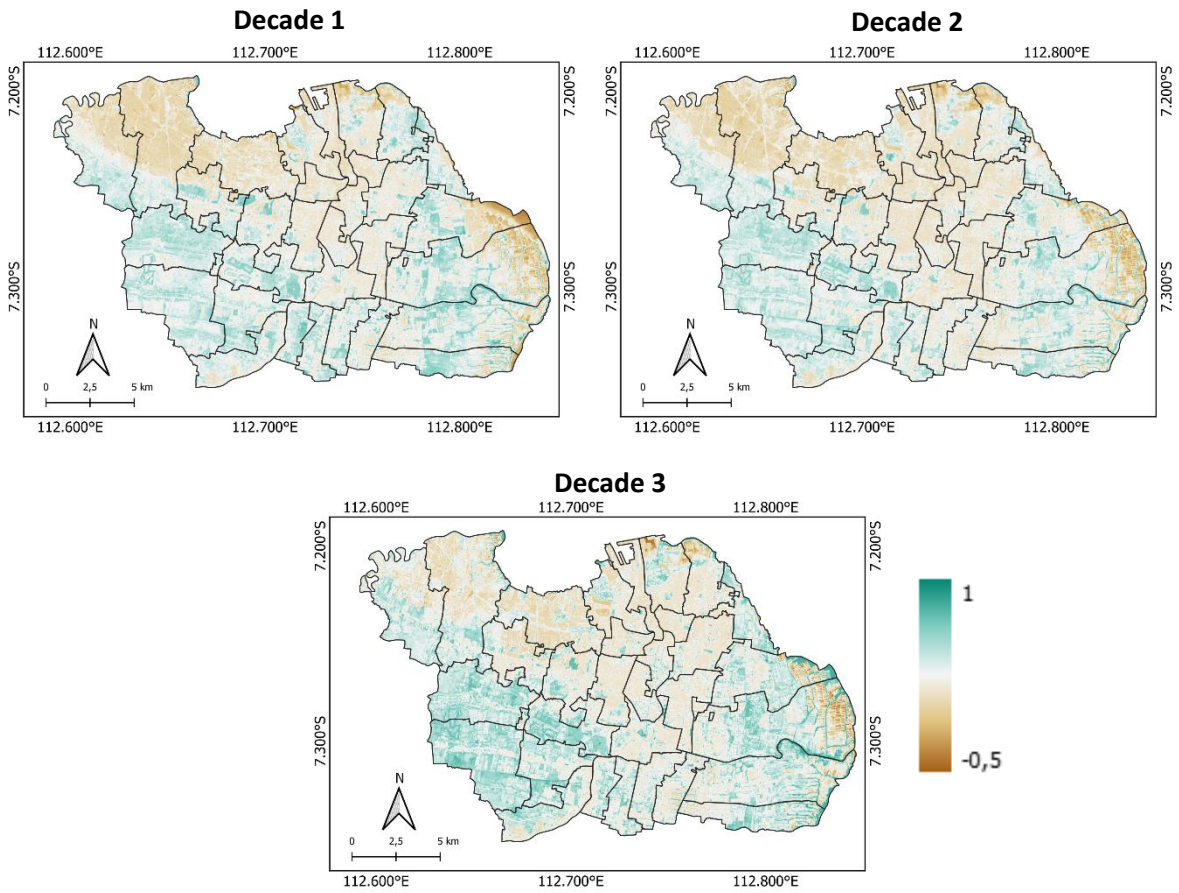

Figure 4. NDVI Spatial Distribution of Surabaya.

Changes in the building area to vegetation are an indication of reforestation in an area, such as the construction of city parks, planting trees on the side of the road, or reforestation in residential areas. Some buildings may have implemented the green roof concept by planting plants on the roof of the building to reduce heat absorption on the surface.

NDVI. Although the NDVI value cannot justify the type of land cover, it can describe the level of vegetation density. The NDVI value of Surabaya in decade 1 has an average value of 0.25 with a maximum value of 0.78 and a minimum of -0.40, then for decade 2 it has an average value of 0.24 with a maximum value of 0.76 and a minimum -0.41, and decade 3 has an average value of 0.29 with a maximum value of 0.84 and a minimum value of -0.52 (Figure 4). The distribution of NDVI with low values in the Surabaya tends to be in the city center and east-north coast areas. The distribution of NDVI values between 3 decades of research time has a similar pattern but differs in the intensity of the values. The eastern Surabaya area which is a water body has an NDVI similar to the downtown area which is a building area. NDVI itself is often used by researchers to describe vegetation in an area [18], [19].

NDBI. The NDBI value which states the level of building density can be used as a choice to describe land cover in an area. This index is quite effective in analyzing buildings in urban areas where there is usually a higher reflectance in the short-wave infrared region, compared to the near-infrared region. The initial NDBI research was developed by Zha who mapped Nanjing, China, and got good results [20]. The Surabaya NDBI value in decade 1 has an average value of -0.09 with a maximum value of 0.36 and a minimum of -0.86, then for decade 2 it has an average value of -0.07 with a maximum value of 0.74 and a minimum of -0.78, and decade 3 has an average value of -0.07 with a maximum value of 0.41 and a minimum of -0.77 (Figure 5). The NDBI pattern between the 3 decades of the study is relatively the same with low values in the eastern and western areas of Surabaya.

LST. Massive infrastructure development in Surabaya causes heat to be trapped and there is an increase in surface temperature. Changes in land cover and use cause energy imbalances in the urban environment, causing severe environmental problems, such as thermal conditions that are harmful to residents. Increasing population density and expanding residential land use exacerbate the UHI phenomenon.

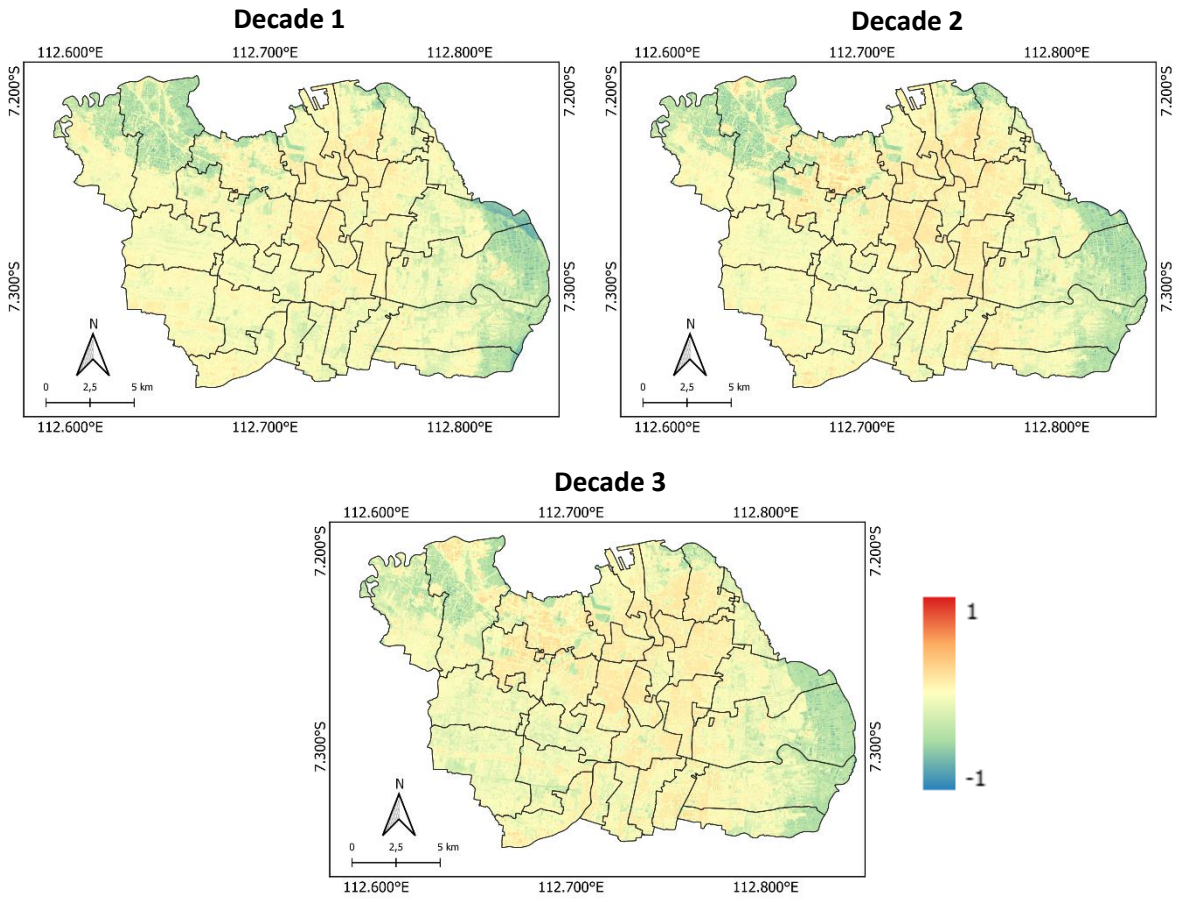

Figure 5. NDBI Spatial Distribution of Surabaya.

The surface temperature was observed to increase significantly in each decade in both the minimum, maximum, and average values (Figure 6). The average surface temperature in the first decade is 27.98ºC with variations ranging from 23.26ºC to 33.06ºC, then for the second decade the average is 29.39ºC with variations ranging from 23.55ºC to 35.98ºC, and in the decade 3 has an average surface temperature of 31.58ºC with variations ranging from 25.54ºC to 36.81ºC. There was an increase in average surface temperature of 1.40ºC between decades 2 and 1, and an increase of 2.19ºC between decades 3 and 2. The increase in surface temperature was centered in the central part of Surabaya. Low Surface Temperatures are observed in areas of the land cover of water bodies and vegetation. Although some areas did not experience land cover changes, they still experienced an average increase of 1.72ºC. This increase occurs because of the impact of global warming which increases the earth's temperature on a wider scale.

Relationship between Land Cover, NDVI, NDBI, and LST. Characteristics of NDVI, NDBI, and LST can be used as an illustration in determining the type of land cover. In this study, it was found that each type of land cover has special characteristics. Based on Figure 7a it can be seen that vegetation has a pattern of high NDVI values, low NDBI, and medium surface temperatures, while buildings have a pattern of low NDVI values, high NDBI, and high surface temperatures, and water bodies have a pattern of medium NDVI values, medium NDBI, and low surface temperature.

The highest average NDVI value is on land cover types of vegetation with a value of 0.517 and the lowest average is on land cover types of buildings with a value of 0.215, while water bodies with an average NDVI value of 0.223. The highest average NDBI value is on land cover types of buildings with a value of 0.038 and the lowest average is on land cover types of water bodies with a value of -0.255, while vegetation with an average NDBI value of -0.160. The highest average surface temperature value is on land cover types of buildings with a value of 32.831ºC and the lowest average is on land cover types of water bodies with a value of 29.095ºC, while vegetation with an average surface temperature of 30,670ºC. The heat gain of buildings is higher than that of vegetation or bodies of water, so the development of infrastructure or settlements will increase the surface temperature in an area. This is in line with the research of Halder, et al (2021), which states that each type of land cover has a different thermal variability [4].

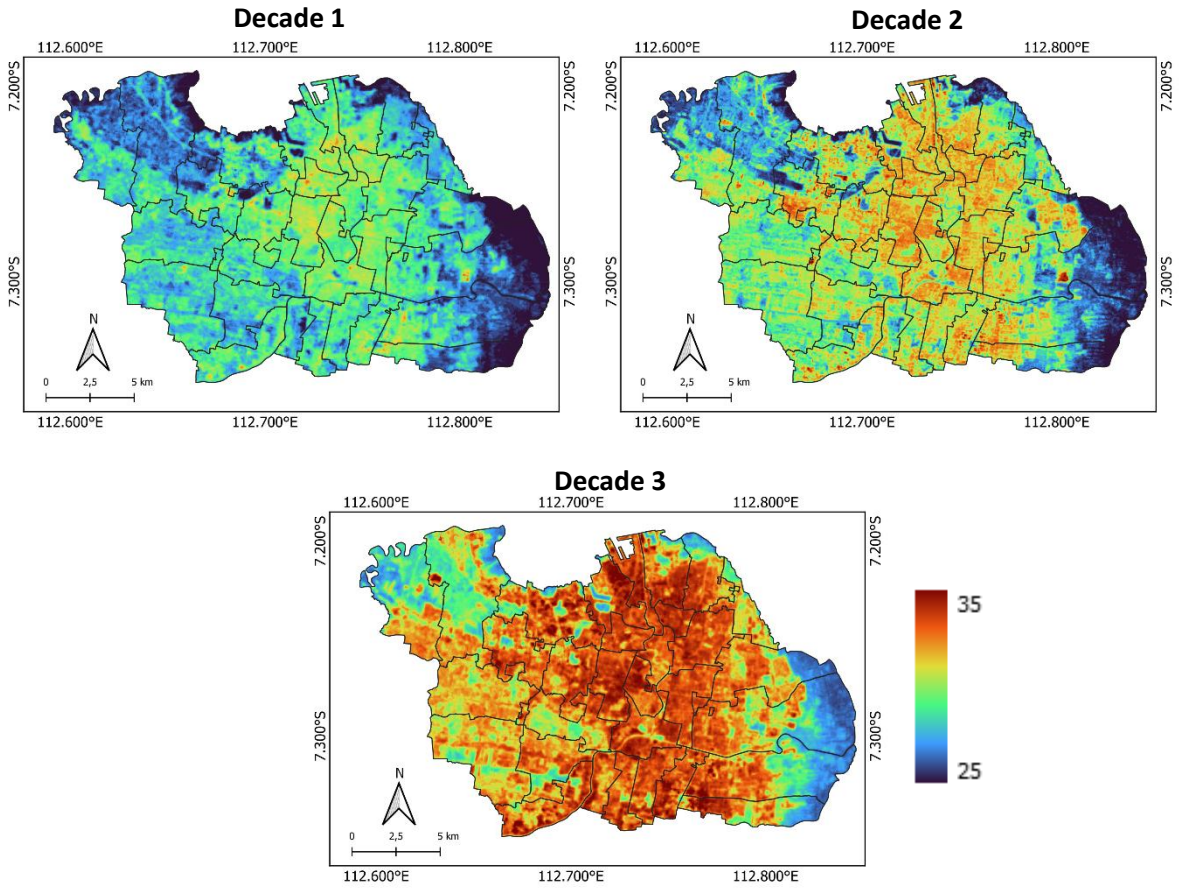

Figure 6. LST Spatial Distribution of Surabaya.

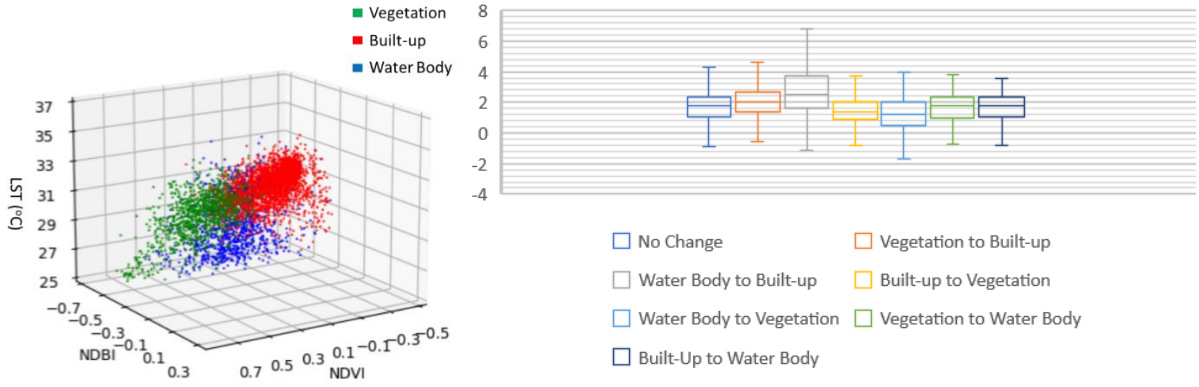

(a) (b)

Figure 7. (a) Scatter plots of NDVI, NDBI, and LST. (b) Impact of Changes in Land Cover on Surface Temperature

The correlation between NDVI and surface temperature shows a negative value with the number -0.31 which means that the addition of vegetation can reduce the surface temperature. On the other hand, the relationship between NDBI and surface temperature shows a positive value of 0.76, which means that an increase in buildings can increase the surface temperature. NDBI is quite strong in describing the pattern of data movement due to the influence of its value on surface temperature compared to NDVI.

Changes in land cover will have an impact on changes in surface temperature for each type of land cover. This is caused by heat reception and different capacities. Changes in land cover from water bodies to buildings have the highest average temperature increase compared to other types with a value of 2.80°C. The lowest change in surface temperature occurred in the type of building land cover to vegetation and water bodies to vegetation with values of 1.40°C and 1.45°C (Figure 7b).

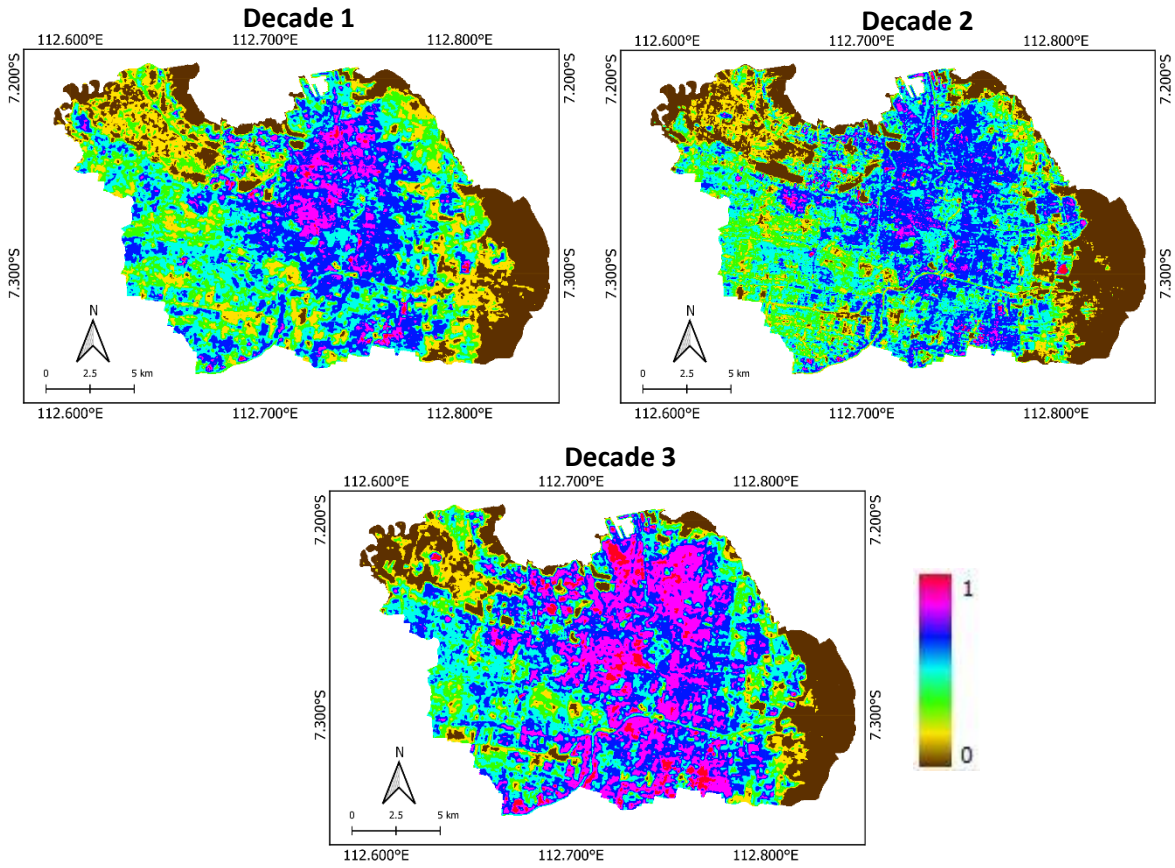

Figure 8. UHI Index Distribution of Surabaya.

UHI. Hot spots in Surabaya were observed as indicated by a UHI index value of more than 0.9 both in decades 1, 2 and 3. The UHI index value was above 0.9 in decade 1, which reached an area of 7.557955 km^2, in decade 2 covering an area of 5.735159 km^2, and in decade 3 that is 12.28253 km^2. In decade 3 there was a significant increase due to a decrease in the amount of vegetation and a significant increase in buildings. Reducing the amount of vegetation will have an impact on climate change. Hotspot occurrences were recorded in the downtown area and several parts of the northern and southern areas (Figure 8). Identification of long-term UHI can be used as planning material in implementing the development and environmental management of the City of Surabaya. Consideration of the increase in surface temperature can encourage the government to use building materials that are low in heat absorption so that it will not further exacerbate the UHI phenomenon. In addition, development planning is recommended vertically upwards to maintain the function of vegetated land. The sky view factor is also an important factor in reducing the impact of UHI where heat will be released into the atmosphere and not retained in the surface area.

4. Conclusion

A decrease in the amount of vegetation (24.3%) and an increase in buildings (29.2%) have been observed in Surabaya from 1991 to 2020 through Landsat satellite imagery, while for water bodies there is an insignificant decrease (4.9%). The existence of a land cover change scheme causes an increase in LST. There has been an increase in LST of 1.4 ^{o}C between decades 1 and 2 and 2.19 ^{o}C between decades 2 and 3. The development of Surabaya started in the downtown area and then developed more dominantly to the west and east. The pattern of urban development is in line with the pattern of changes in LST that occur. The highest change in land cover type during the study period was the change in vegetation to buildings.

NDVI and NDBI are considered quite good in describing the level of vegetation and building density in an area associated with LST patterns. Of the three types of land cover, buildings have the highest surface temperature, then vegetation, and water bodies. Changes in land cover from water bodies to buildings show the highest increase in surface temperature compared to other land cover changes which can exacerbate the UHI phenomenon. A significant increase in hotspots occurred in decade 3 as indicated by a high UHI index in Surabaya. UHI can increase the impact of climate change in urban areas because there are changes in atmospheric and surface conditions.

References

[1] S. Sultana and A. N. V. Satyanarayana, "Urban heat island intensity during winter over metropolitan cities of India using remote-sensing techniques: impact of urbanization," *Int J Remote Sens*, vol. 39, no. 20, pp. 6692–6730, Oct. 2018, doi: 10.1080/01431161.2018.1466072.

[2] R. Bala, R. Prasad, and V. P. Yadav, "Quantification of urban heat intensity with land use/land cover changes using Landsat satellite data over urban landscapes," *Theor Appl Climatol*, vol. 145, no. 1–2, pp. 1–12, Jul. 2021, doi: 10.1007/s00704-021-03610-3.

[3] Y. Chen and S. Yu, "Impacts of urban landscape patterns on urban thermal variations in Guangzhou, China," *International Journal of Applied Earth Observation and Geoinformation*, vol. 54, pp. 65–71, Feb. 2017, doi: 10.1016/j.jag.2016.09.007.

[4] B. Halder, J. Bandyopadhyay, and P. Banik, "Monitoring the effect of urban development on urban heat island based on remote sensing and geo-spatial approach in Kolkata and adjacent areas, India," *Sustain Cities Soc*, vol. 74, p. 103186, Nov. 2021, doi: 10.1016/j.scs.2021.103186.

[5] Y. Li, H. Zhang, and W. Kainz, "Monitoring patterns of urban heat islands of the fast-growing Shanghai metropolis, China: Using time-series of Landsat TM/ETM+ data," *International Journal of Applied Earth Observation and Geoinformation*, vol. 19, pp. 127–138, Oct. 2012, doi: 10.1016/j.jag.2012.05.001.

[6] S. Sultana and A. N. V. Satyanarayana, "Assessment of urbanisation and urban heat island intensities using landsat imageries during 2000 – 2018 over a sub-tropical Indian City," *Sustain Cities Soc*, vol. 52, p. 101846, Jan. 2020, doi: 10.1016/j.scs.2019.101846.

[7] H. Kandel, A. Melesse, and D. Whitman, "An analysis on the urban heat island effect using radiosonde profiles and Landsat imagery with ground meteorological data in South Florida," *Int J Remote Sens*, vol. 37, no. 10, pp. 2313–2337, May 2016, doi: 10.1080/01431161.2016.1176270.

[8] L. Yang, F. Qian, D.-X. Song, and K.-J. Zheng, "Research on Urban Heat-Island Effect," *Procedia Eng*, vol. 169, pp. 11–18, 2016, doi: 10.1016/j.proeng.2016.10.002.

[9] J. A. I. Paski, F. Alfahmi, D. S. Permana, and E. E. S. Makmur, "Reconstruction of Extreme Rainfall Event on September 19-20, 2017, Using a Weather Radar in Bengkulu of Sumatra Island," *The Scientific World Journal*, vol. 2020, pp. 1–6, Jul. 2020, doi: 10.1155/2020/1639054.

[10] Md. N. Rahman *et al.*, "Impact of Urbanization on Urban Heat Island Intensity in Major Districts of Bangladesh Using Remote Sensing and Geo-Spatial Tools," *Climate*, vol. 10, no. 1, p. 3, Jan. 2022, doi: 10.3390/cli10010003.

[11] N. Ullah, M. A. Siddique, M. Ding, S. Grigoryan, T. Zhang, and Y. Hu, "Spatiotemporal Impact of Urbanization on Urban Heat Island and Urban Thermal Field Variance Index of Tianjin City, China," *Buildings*, vol. 12, no. 4, p. 399, Mar. 2022, doi: 10.3390/buildings12040399.

[12] A. Amindin, S. Pouyan, H. R. Pourghasemi, S. Yousefi, and J. P. Tiefenbacher, "Spatial and temporal analysis of urban heat island using Landsat satellite images," *Environmental Science and Pollution Research*, vol. 28, no. 30, pp. 41439–41450, Aug. 2021, doi: 10.1007/s11356-021-13693-0.

[13] R. C. Estoque, Y. Murayama, and S. W. Myint, "Effects of landscape composition and pattern on land surface temperature: An urban heat island study in the megacities of Southeast Asia," *Science of The Total Environment*, vol. 577, pp. 349–359, Jan. 2017, doi: 10.1016/j.scitotenv.2016.10.195.

[14] N. Kikon, P. Singh, S. K. Singh, and A. Vyas, "Assessment of urban heat islands (UHI) of Noida City, India using multi-temporal satellite data," *Sustain Cities Soc*, vol. 22, pp. 19–28, Apr. 2016, doi: 10.1016/j.scs.2016.01.005.

[15] L. de F. Peres, A. J. de Lucena, O. C. Rotunno Filho, and J. R. de A. França, "The urban heat island in Rio de Janeiro, Brazil, in the last 30 years using remote sensing data," *International Journal of Applied Earth Observation and Geoinformation*, vol. 64, pp. 104–116, 2018, doi: 10.1016/j.jag.2017.08.012.

[16] S. Sultana and A. N. V. Satyanarayana, "Assessment of urbanisation and urban heat island intensities using landsat imageries during 2000 – 2018 over a sub-tropical Indian City," *Sustain Cities Soc*, vol. 52, Jan. 2020, doi: 10.1016/j.scs.2019.101846.

[17] N. Speybroeck, "Classification and regression trees," *Int J Public Health*, vol. 57, no. 1, pp. 243–246, 2012, doi: 10.1007/s00038-011-0315-z.

[18] A. Majkowska, L. Kolendowicz, M. Półrolniczak, J. Hauke, and B. Czernecki, "The urban heat island in the city of Poznań as derived from Landsat 5 TM," *Theor Appl Climatol*, vol. 128, no. 3–4, pp. 769–783, May 2017, doi: 10.1007/s00704-016-1737-6.

[19] M. Ranagalage, R. C. Estoque, and Y. Murayama, "An Urban Heat Island Study of the Colombo Metropolitan Area, Sri Lanka, Based on Landsat Data (1997–2017)," *ISPRS Int J Geoinf*, vol. 6, no. 7, p. 189, Jun. 2017, doi: 10.3390/ijgi6070189.

[20] Y. Zha, J. Gao, and S. Ni, "Use of normalized difference built-up index in automatically mapping urban areas from TM imagery," *Int J Remote Sens*, vol. 24, no. 3, pp. 583–594, Jan. 2003, doi: 10.1080/01431160304987.